Theory of the Effects of Rapid Thermal Annealing on Thin-Film Crystallization

E. K. F. Dang and R. J. Gooding
Department of Physics, Queen's University, Kingston, Ontario, Canada K7L 3N6
(Received 2 August 1994)

The crystallization of amorphous thin films by annealing can sometimes be greatly aided by rapidly bringing the films up to the annealing temperature, so-called rapid thermal annealing (RTA). We have modeled this phenomenon for lead zirconate titanate thin films, incorporating the presence of a long-lived secondary crystalline state, and have studied the approach to steady state using Langevin simulations. We find that one can accurately model this RTA process only when one includes the long-ranged interactions expected to be generated by elastic misfits of the inhomogeneous intermediate state.

PACS numbers: 64.70.Dv, 68.55.–a, 77.55.+f, 77.84.Dy

It is well-established experimentally [1] that many amorphous thin films can be crystallized in an expedient manner through the use of rapid thermal annealing (RTA). One of the crystallization transformations that has attracted attention is that undergone by the ferroelectric lead zirconate titanate (PZT). Here, we present a simple model of this particular transition to demonstrate some intriguing features of RTA.

The interests in PZT, and other ferroelectric ceramic thin films, arise because of their important potential applications. Attempts have thus been made in developing reliable fabrication techniques of these films [2–5]. In all of the deposition processes commonly used, such as metal-organic chemical-vapor deposition, dc and rf magnetic sputtering, and sol-gel processing, the as-deposited films are amorphous and nonferroelectric. Postdeposition annealing treatments are required to enable the films to crystallize into a ferroelectric perovskite structure. Conventional furnace annealing (CFA) typically involves heating rates of order $1-10\,^{\circ}\mathrm{C/s}$, with final temperatures of about 600 °C, and annealing times of the order of 1 h. However, since many of the technological applications of ferroelectric ceramics films demand successful integration of the films into semiconductor devices, it is crucial to reduce either the annealing temperature or annealing time, or both, in order to avoid strains and other defects at the film-substrate interface [6]. In this respect, RTA, as characterized by an extremely large heating rate (e.g., 100 °C/s), has been shown to achieve these criteria [3–5].

A comprehensive theoretical understanding of the differences between CFA and RTA, or, more precisely, of the role of heating rates in the crystallization of PZT, will involve a detailed study of the chemical and structural transformation path that begins with the amorphous film and ends with the final perovskite structure. However, it is also useful, in the first instance, to investigate the process in terms of a simple phenomenological model with the aim of identifying the essential physics involved. Here we present such an investigation using a Landau model and Langevin dynamical simulations. The Landau potential is an effective free energy functional determined by a small number of order parameters, such that it represents the competition between locally stable phases. Our model involves a single scalar field and incorporates the possibility that the transformation proceeds via an intermediate defect-pyrochlore state, such as was observed in CFA experiments [2,4,5,7,8]. We have found that a necessary feature of a model which successfully accounts for the observed experimental behavior involves long-ranged elastic interactions. We have chosen a simple potential to represent this effect, as motivated by the work of Littlewood and Chandra [9], who showed that long-ranged elastic forces produce a well-defined delay time in nucleation and growth processes, in good agreement with experimental results [10] for ferroelectric barium titanate ($BaTiO_3$).

First, let us clearly review the experimental data which has piqued our interest. In experiments the composition of the PZT films is routinely determined by x-ray diffraction. In addition, since the dielectric constants of both the amorphous and defect-pyrochlore phases are about 60, while that of the perovskite is almost 1400, dielectric measurements offer a good indication of the fraction of the film that has transformed to the ferroelectric perovskite phase [5]. It is well known that in CFA the composition and structure of the ceramics PZT film depend strongly on both the annealing temperature and annealing time [2,3,5,7,8]. At intermediate annealing temperatures, in the region of 450–600 °C, the resulting film predominantly consists of the defect-pyrochlore [$Pb_2(Zr/Ti)_2O_6$] phase. Above 600 °C, the system starts to transform to the perovskite [$Pb(Zr/Ti)O_3$] phase. Even at such high temperatures, the transformation is still not entirely complete after soaking for 1 h.

Martin [8] suggested that a reason why the defect-pyrochlore structure tends to be formed as an intermediate phase is that the perovskite system is a very dense structure, in comparison to the more open, less dense defect-pyrochlore phase. Indeed, one might expect the less dense material to be more readily formed from the amorphous phase. However, we believe that there

 0031-9007/95/74(19)/3848(4)$06.00

is a second reason for the presence of an intermediate defect-pyrochlore state: It is well known [4,11] that one must have a certain abundance of lead for the formation of perovskite to proceed. We believe that this may be attributed to the formation of lead oxide from the perfect pyrochlore state, the former being found in abundance after the transition has been completed [11]. Schematically, this corresponds to

$$\text{excess Pb} + \text{Pb}_2(\text{Zr/Ti})_2\text{O}_7 \rightarrow \text{excess PbO} + \text{Pb}_2(\text{Zr/Ti})_2\text{O}_6 . \quad (1)$$

Then, having obtained an intermediate (defect-pyrochlore) state which has an *identical* stoichiometry to that of the desired cubic perovskite, the final transition can be completed without any diffusion [12].

RTA processing, which utilizes a heating rate of about 100 °C/s, leads to crystallization kinetics that are strikingly different than CFA. The essential differences between CFA and RTA, as observed, e.g., by Hu, Peng, and Krupanidhi [5], are twofold. Observation 1: In RTA, the defect-pyrochlore phase starts to form at a lower temperature, about 340 °C, and the perovskite phase forms above 415 °C. Observation 2: With RTA, for all annealing temperatures above 450 °C, the transformation to perovskite is very rapid, achieving complete transition with a soaking time of *only* one second. Wu *et al.* [3] also investigated the RTA process as a function of heating rates. Their results support the notion that an increase in heating rate reduces both the annealing temperature and time required for transformation to the perovskite.

Based on their observations, Hu, Peng, and Krupanidhi [5] suggested that in CFA, the complete transformation of the PZT film is a three-stage process. First, the amorphous film undergoes some type of relaxation process, which is strongly exothermic. The relaxed amorphous film then transforms to the metastable defect-pyrochlore phase. Finally, the film transforms to the stable perovskite phase. When the heating is slow, the heat released in the relaxation of the amorphous film is slowly dispersed, and plays no role in the crystallization process. In RTA, however, the rapid increase in temperature means that defect-pyrochlore formation may be *bypassed*. Furthermore, the heat released in the relaxation process is not dispersed, but aids in further nucleation and crystallization of the perovskite phase. This accounts for the fact that the films produced via RTA crystallize both faster and also at a lower temperature than in CFA.

We now present an alternative model that is significantly different from the above picture. Specifically, we do not attempt to exclude the defect-pyrochlore phase from the transition path. Rather, we rely on enhanced *fluctuations*, viz., we drive the system toward equilibrium with rapidly elevated temperatures as in RTA. The model we propose is described by a Landau-type free energy that is a functional of a single scalar field, $\psi = \{\psi_i\}$, where the subscript i denotes sites on a $L \times L$ lattice, and $-\infty < \psi_i < \infty$:

$$\mathcal{F}[\psi] = \sum_i \{V(\psi_i) + \tfrac{1}{2}K(\nabla\psi_i)^2 + \tfrac{1}{2}\ell(\psi_i - \overline{\psi})^2\}. \quad (2)$$

The first term $V(\psi_i)$ in the summation in Eq. (2) is a one-dimensional potential. Its precise form is discussed below. The second term is the discrete version of the squared gradient. Via the third term, a long-ranged interaction is also introduced, intended to mimic the elastic forces that arise from the presence of deformed inhomogeneities [13] in a mean-field manner [9]. Here, $\overline{\psi} = (1/L^2)\sum_j \psi_j$ is the spatial average of the order parameter, and ℓ is the strength of this interaction.

The potential $V(\psi_i)$ that we have considered has a three-well structure. For simplicity of implementation we consider a piecewise quadratic form (Fig. 1). Physically, we associate the wells at A, B, and C with the defect-pyrochlore, amorphous, and perovskite phases, respectively. We are interested in the following conditions:

$$V_D < V_E \quad (3)$$

and

$$V_C < V_A < V_B . \quad (4)$$

The rationale for choosing this particular form of the potential is as follows. Equation (3) means that the energy barrier relevant to the transition from the phase B to the phase A is lower than that for the transition from phase B to phase C—such barriers, and the relative magnitudes of these barriers, are consistent with observation 1. The second condition, Eq. (4), defines phase C as the ground state, while phases A and B are metastable local energy minima. If, at some initial time, the system was in well B, this model represents two competing phases (A and C) into which the initial high energy phase (B) may transform. Because of the lower energy barrier, $V_D - V_B$ compared with $V_E - V_B$, initially more of the system will transform to A. However, the lower free energy of C means that eventually this will be the dominant phase.

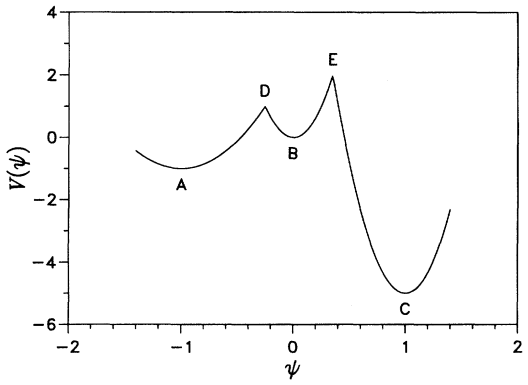

FIG. 1. A piecewise quadratic potential with three energy minima. The A, B, and C wells are taken to represent the defect-pyrochlore, amorphous, and perovskite phases, respectively.

The dynamical evolution from an arbitrary initial configuration toward equilibrium can be generated by a Langevin equation:

$$\frac{d\psi_i}{dt} = -\Gamma \frac{\delta \mathcal{F}[\psi]}{\delta \psi_i} + \eta_i(t). \quad (5)$$

Here Γ is a kinetic coefficient and η_i is a Gaussian thermal noise with zero mean satisfying the ensemble average

$$\langle \eta_i(t)\ \eta_j(t') \rangle = 2\Gamma k_B T \delta_{ij} \delta(t - t'). \quad (6)$$

Note that in the present study, temperature is introduced into the model *solely* via the stochastic thermal noise—the Landau free energy (2) is temperature independent.

The simplest numerical procedure to solve Eq. (5) is given by the Euler method [14]. In this algorithm, time is discretized into steps of the size δt. After substituting the free energy $\mathcal{F}[\psi]$, as given by Eq. (2), into the Langevin equation (5), and rescaling the variables appropriately, we obtain

$$\psi_i(t + \delta t) = \psi_i(t) + \delta t \left\{ -\frac{d\tilde{V}(\psi_i)}{d\psi_i} + \tilde{K} \sum_{\mathbf{a}} (\psi_{i+\mathbf{a}} - \psi_i) - \tilde{\ell}(\psi_i - \overline{\psi}) \right\} + \sqrt{2\delta t}\, \xi_i(t), \quad (7)$$

where $\mathbf{a}$ is a nearest neighbor lattice vector, and $\xi_i(t)$ satisfies

$$\langle \xi_i(t)\ \xi_j(t') \rangle = \epsilon \delta_{ij} \delta_{tt'}.$$

Here, ϵ is the scaled temperature in dimensionless units. All other quantities including the time t, the potential $\tilde{V}$, and the coupling constants $\tilde{K}$ and $\tilde{\ell}$ are also dimensionless. From this equation we see that the long-ranged interaction manifests itself as a field, dependent upon the average state of the entire system [9].

In RTA, the sample temperature is typically computer controlled to maintain a constant heating rate up to annealing [15]. To mimic this experimental situation in our simulations, we let the scaled temperature ϵ increase linearly from zero to the annealing temperature, which we denote by ϵ_a, and then fix the temperature at this value for the remainder of the simulation. While one might anticipate the equilibrium expectation values to be determined solely by the annealing temperature, our simulations demonstrate that the competing intermediate metastable phases actually play an important role. We have carried out simulations on a variety of lattice sizes with periodic boundary conditions, as well as run many different thermal fluctuation force sequences, and have obtained converged values of the averaged order parameter $\langle \psi \rangle$ at each instant in time. In principle, a quantitative comparison with experiments is possible if the relative magnitudes of the barrier heights for the respective transformations, i.e., amorphous pyrochlore and amorphous perovskite, are known. While to our knowledge such data are not fully available in the literature, these could be obtained, for example, through an Avrami analysis using either an x-ray diffraction [16] or scanning electron microscopy [17] approach. For the results described below, we have chosen for the potential parameters $(\tilde{V}_A, \tilde{V}_B, \tilde{V}_C, \tilde{V}_D, \tilde{V}_E) = (-1, 0, -5, 1, 2)$, $(\psi_A, \psi_B, \psi_C, \psi_D, \psi_E) = (-1, 0, +1, -0.2, 0.2\sqrt{2})$, and $\tilde{K} = 0.1$, consistent with Eqs. (3) and (4). All our simulations begin with the entire system localized in the B well.

When no long-ranged interaction is included ($\tilde{\ell} = 0$), evolutions similar to those shown in the inset of Fig. 2 are obtained. For this system one finds that although the very short time dynamics are a function of the heating rate, the equilibrium average is not, showing that the true equilibrium states are accessed in all cases. This behavior is widely different from that of the experiments.

When long-ranged interactions are included ($\tilde{\ell} \neq 0$), we have determined the long-time averages of the order parameter as a function of both the annealing temperature and heating rate. This allows us to make a qualitative comparison to the measurements of the normalized x-ray intensities shown in Fig. 4 of Ref. [3], and to the dielectric constant data shown in Fig. 6 of Ref. [5]. Our Fig. 2 shows that for $\tilde{\ell} = 5$, a change in the heating rate by a factor of 2 can lead to very different long-time averages, in contrast to the $\tilde{\ell} = 0$ behavior. We find that, as shown in Fig. 3, the transition to the true equilibrium state starts to occur at a lower annealing temperature in the case of a higher heating rate. Furthermore, there exists a range of ϵ_a (from 0.8 to 1.4) over which the faster heating rate leads to a completed transition, whereas the slower heating rate leads to incomplete formation of the perovskite phase. The larger the difference in heating rates, the more pronounced this difference becomes. Clearly, these trends are similar to the experimental results (see observation 1). (From the dielectric measurements of Ref. [5], with RTA,

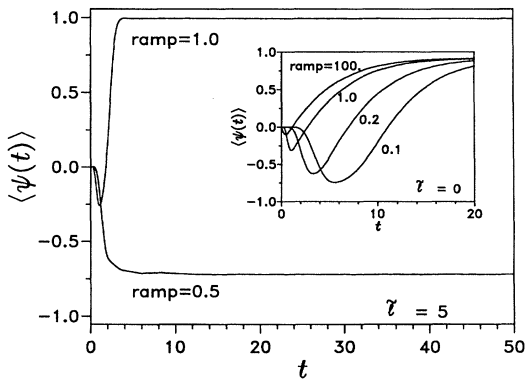

FIG. 2. The time evolution of the order parameter for $\tilde{\ell} = 5$ and $\tilde{\ell} = 0$ (inset), plotted for the various ramp rates shown. For both sets of simulation, $\epsilon_a = 1.0$. For $\tilde{\ell} = 5$ and 0, averages are performed over 400 and 40 different random force sequences, respectively. The inverse of the ramp rate shown is equal to the number of time units before the annealing temperature $\epsilon_a = 1$ is reached.

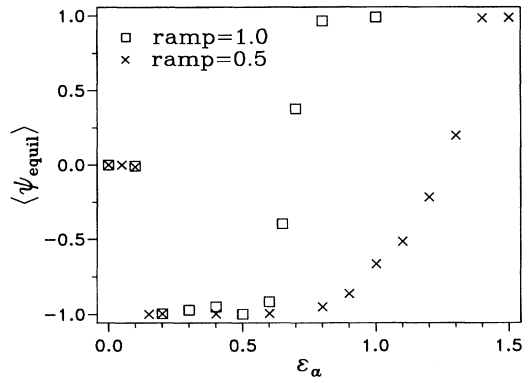

FIG. 3. The long-time asymptotic limit of the average order parameter $\langle\psi_{equil}\rangle$ as a function of the annealing temperature, plotted for two ramp rates, with long-ranged interaction $\tilde{\ell} = 5$.

the transition to perovskite starts to occur around 415 °C, and is completed by 450 °C. With CFA, the transition only begins above 600 °C, and is not totally complete even at 700 °C. Indeed, one can reproduce these numerical values with an appropriate choice of $\tilde{\ell}$; however, as we discuss later, we believe that such quantitative comparisons are premature.)

We now propose a simple explanation of our simulation results. The significance of the long-ranged interaction in our model is that it imposes an effective bias field that is proportional to the average order parameter $\langle\psi\rangle$. Consider first the results of the inset of Fig. 2 for which long-ranged interaction is absent. Each curve in the figure demonstrates the competition between the metastable phase $\psi_A = -1$ and the true ground state $\psi_C = +1$. As the ramp rate is reduced, it takes a longer time for thermal fluctuations to reach large enough amplitudes to overcome the large energy barrier to the ground state C. Therefore, initially, a larger fraction of the system is transformed to phase A, resulting in a more negative value of the average order parameter $\langle\psi\rangle$, as shown in the figure.

When the long-ranged interaction is included, a larger negative $\langle\psi\rangle$ produces a stronger negative bias, so that the system is much more likely to be trapped in the metastable state. This provides a clear explanation of why a higher annealing temperature is required for transformation to the stable state (Fig. 3). Physically, when either the defect-pyrochlore or perovskite phase nucleates in the material, elastic forces favor the transformation of the rest of the system to the same phase. In the present mean-field description of the long-ranged forces, the overall bias is toward the competing phase that initially exists in a larger fraction. Although the defect pyrochlore is thermodynamically less favorable compared with the perovskite, kinetically it is more accessible from the amorphous phase. With a slow heating rate, therefore, the relative ease of defect-pyrochlore formation results in it being the dominant product phase up to a higher annealing temperature.

The simple model presented here shows how the heating rate, which underlies the difference between CFA and RTA, can drastically affect PZT crystallization through the competition between metastable phases—this latter effect is enhanced by long-ranged elastic interactions. For a quantitative comparison between simulations and experiments, it is clear that our 1D Landau potential should be changed to something more physically representative of the transitions undergone between the various structures found in the formation of PZT. We have recently completed such an extension based on a density-wave expansion (in preparation). In this way, the usefulness of RTA with regards to a particular material's processing history can be determined theoretically.

We are grateful to Mike Sayer, Ellen Griswold, and David Barrow for helpful comments on the experimental details of this problem. This work was supported by the OCMR, an Ontario Centre for Excellence.

[1] See, e.g., *Rapid Thermal and Integrated Processing II,* MRS Symposia Proceedings No. 303 (Materials Research Society, Pittsburgh, 1993).
[2] C. V. R. Vasant Kumar *et al.,* Appl. Phys. Lett. **58**, 1161 (1991).
[3] Z. Wu *et al.,* Mater. Res. Soc. Symp. Proc. **224**, 305 (1991).
[4] C. V. R. Vasant Kumar, R. Pascual, and M. Sayer, J. Appl. Phys. **71**, 864 (1992).
[5] H. Hu, C. J. Peng, and S. B. Krupanidhi, Thin Solid Films **223**, 327 (1993).
[6] For example, see K. Sreenivas *et al.,* in *Ferroelectric Thin Films,* edited by E. R. Myers and A. I. Kingon, MRS Symposia Proceedings No. 200 (Materials Research Society, Pittsburgh, 1990), p. 255; Z. Wu and M. Sayer, in Proceedings of the 8th International Symposium on Applications of Ferroelectrics (unpublished).
[7] A. Okada, J. Appl. Phys. **49**, 4495 (1978).
[8] F. W. Martin, Phys. Chem. Glasses **6**, 143 (1965).
[9] P. B. Littlewood and P. Chandra, Phys. Rev. Lett. **57**, 2415 (1986); P. Chandra, Phys. Rev. A **39**, 3672 (1989).
[10] D. B. McWhan *et al.,* J. Phys. C **18**, 1307 (1985); D. A. Neumann *et al.,* Phys. Rev. B **32**, 1866 (1985).
[11] M. Klee *et al.,* J. Appl. Phys. **72**, 1566 (1992).
[12] The details of the continuous crystallographic transformation path connecting the two crystalline phases will be discussed elsewhere.
[13] J. D. Eshelby, Proc. R. Soc. London A **241**, 376 (1957); A. C. E. Reid and R. J. Gooding, Phys. Rev. B **46**, 6045 (1992).
[14] O. T. Valls and G. F. Mazenko, Phys. Rev. B **34**, 7941 (1986); **42**, 6614 (1990).
[15] M. Sayer *et al.,* J. Can. Ceram. Soc. **62**, 63 (1993).
[16] A. P. Wilkinson *et al.,* Chem. Mater. **6**, 750 (1994).
[17] C. K. Kwok and S. B. Desu, J. Mater. Res. **9**, 1728 (1994).